2014

Modeling of a Hot Gas Bypass Test Block for Centrifugal Compressors

Paul D. Gessler
Marquette University, United States of America, paul.gessler@marquette.edu

Margaret M. Mathison
Marquette University, United States of America, margaret.mathison@marquette.edu

Anthony J. Bowman
Marquette University, United States of America, anthony.bowman@marquette.edu

Modeling of a Hot Gas Bypass Test Block for Centrifugal Compressors

Paul D. Gessler[1*], Margaret M. Mathison[1], Anthony J. Bowman[1]

[1] Marquette University, Department of Mechanical Engineering,
Milwaukee, Wisconsin, USA

* Corresponding Author
Email: paul.gessler@marquette.edu, Phone: (414) 241-1627

ABSTRACT

The increasingly competitive building equipment and control industry pushes manufacturers to continually improve the performance and efficiency of their products to develop and maintain a competitive edge. Compressor development is an expensive endeavor, but the cost and time required for testing can be minimized by developing a model of the compressor test block to predict its behavior with a given prototype compressor at specified operating conditions. This paper presents a thermodynamic model of a hot gas bypass test block used to evaluate centrifugal compressor performance at a compressor development facility.

The test block uses cooling towers to reject the heat of compression to outdoor air, and experience has shown that the range of achievable compressor test conditions can be limited by outdoor air temperature and humidity, which affect the heat transfer rate. Therefore, one goal of the model development was to provide a means for evaluating the feasibility of tests at given outdoor air conditions. A second goal of the model was to assist in selecting the orifice plate used in the orifice flow meter that measures mass flow through the compressor.

The model assumes that the system operates at steady-state conditions and uses a compressor map to model expected prototype compressor performance. Therefore, this research focuses on the condenser and cooling tower models, which are the most important elements for predicting the impact of outdoor conditions on cycle performance. It is shown that the resulting model achieves agreement to within 2.5% of experimental data. The results for orifice differential pressure agree to within 0.35% of experimental data, providing a useful orifice selection routine.

1. INTRODUCTION

Minimizing compressor testing time has a large impact on development costs and time to market. A test block model based on first principles has the potential to reduce the testing time and thus decrease costs by assisting the test engineer in defining an optimized test plan built around test block capabilities at the expected ambient conditions. Furthermore, the downtime for changing flow measurement orifices can be minimized by providing a means to choose the best orifice diameter for a given range of test flow rates.

With these considerations in mind, the overall goal of this research was to create a thermodynamic model to simulate the 1.1 MW gas block compressor testing equipment used by the project sponsor. This equipment uses a hot gas bypass (HGBP) cycle to simulate the compressor operating conditions of the actual refrigeration cycle without requiring an evaporator or associated cooling load. The primary refrigerant used in this system is R-134a, but the equipment allows for a wide variety of refrigerants to be used, as does the thermodynamic model.

The model will use the design conditions of the new compressor (mass flow, pressure head, shaft speed, and isentropic/map efficiency) to determine the test block setup (flow measurement orifice size and cooling tower fan speed) required to conduct tests at given ambient conditions. The current testing process requires some trial and error to find a suitable test block setup for a new compressor. The thermodynamic model aims to quickly provide reasonably accurate initial estimates of the orifice diameter and cooling tower fan speed required to test a new compressor at specified outdoor air conditions. Therefore, the testing time is reduced by eliminating (or at least minimizing) the trial and error phase of the testing process.

The equipment and configuration of a typical hot gas bypass test block cycle is described thoroughly in existing literature, primarily in work by McGovern (1984), Dirlea et al. (1996), and Sahs and Mould (1956). Thermodynamic models of the individual components in the test block cycle exist, are well-established, and are used frequently in the thermal

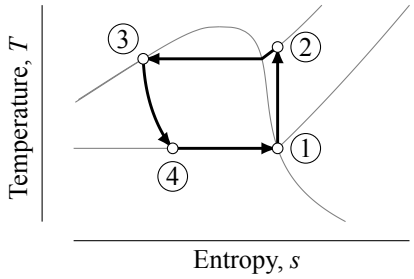

(a) Vapor-compression refrigeration cycle.

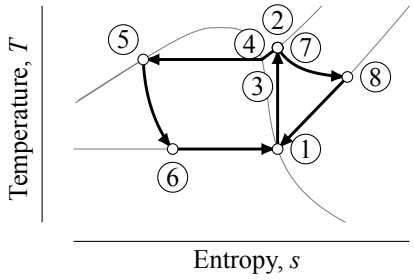

(b) Hot gas bypass cycle.

Figure 1: Comparison of idealized temperature-entropy (*T*-*s*) diagrams.

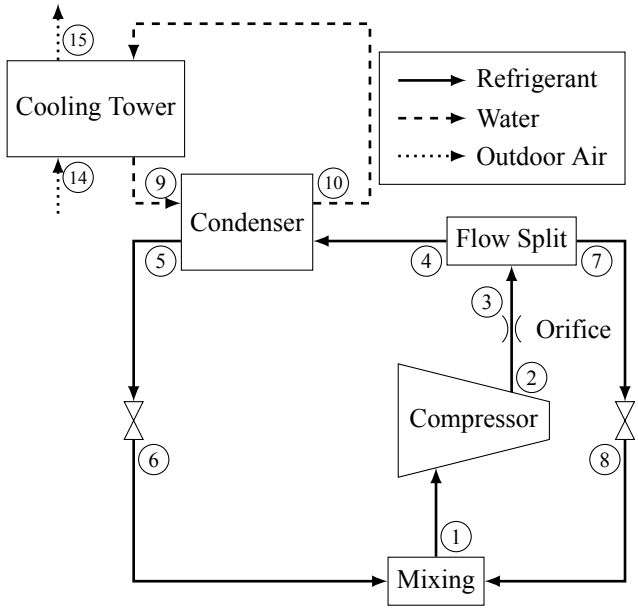

Figure 2: Simplified schematic of the gas test block facility.

and fluid sciences. The novelty of this work is not derived from breakthroughs in the modeling theory surrounding the components, but rather from an integration of existing models into a comprehensive tool at an appropriate level for use in industry applications. Its significance may be measured by the impact on the daily workflow of test engineers in the compressor development group.

1.1 Background

A preferred method of evaluating compressor performance is to test the compressor on a closed-loop gas test block using the design process fluid (refrigerant) at design flow conditions. While the equipment can be expensive to construct, operate, and maintain, the gas test block makes isolating the compression portion of the refrigeration cycle easier. The basic premise of the gas test block cycle is that the cycle can maintain conditions at the compressor inlet similar to those experienced in a traditional vapor-compression refrigeration cycle, while the conditions at other points in the cycle need not follow the traditional refrigeration cycle arrangement. Temperature-entropy (*T*-*s*) diagrams for the typical vapor-compression refrigeration cycle and an idealized gas block test cycle are shown in Fig. 1, with process 1–2 representing the ideal, isentropic compression process for both cycles. A simplified schematic of the test block layout is shown in Fig. 2, with state numbering corresponding to Fig. 1b.

1.2 Objectives

The overall goal of this research is to develop a one-dimensional, steady-flow thermodynamic model representing the 1.1 MW gas test block at the project sponsor's testing facility. The numerical model will be used in conjunction with compressor maps and/or computational fluid dynamics (CFD) models of the compressors to quantitatively predict the performance of new compressor designs on the test block. To accomplish the overall goal and satisfy the needs of the project sponsor (Iancu, 2012), the model must compute the power requirements for the prime mover of the test block, choose the orifice diameter that results in the smallest error in measured flow rate over the desired range of operating conditions, and report the limits of the test block operating conditions for a given compressor design, test block control settings, and ambient air conditions.

1.3 Requirements and Constraints

The numerical model must be straightforward for engineers in the compressor engineering group to use and update and should minimize dependencies on licensed software for better portability. The software tools generally available to the

compressor engineering group are Engineering Equation Solver (EES) and MATLAB/Simulink. Engineering Equation Solver was chosen since the engineers are more familiar with EES, and EES has built-in thermophysical property relations while MATLAB/Simulink requires interfacing with an external library.

The execution time of the model should be less than one minute for each individual compressor test. Output variables concerning the compressor and flow measurement orifice must not deviate from experimental results by more than 5%. At other areas in the cycle, such as at the condenser and cooling tower, a maximum deviation of 10% is required.

2. THEORETICAL MODEL DEVELOPMENT

This section presents the development of the equations used to model the compressor test block from first principles. Section 2.1 contains the general mass and energy balance equations, to which the appropriate assumptions for each device in the cycle are applied to produce the device-specific equations, as detailed in Sections 2.2 to 2.6. Subscripts i and o are used to indicate the inlet and outlet states of the device, respectively.

2.1 General Balance Equations

The rate forms of the balance equations are used throughout the model. This section lists the mass and energy balances (Çengel and Boles, 2011) with several model-wide assumptions applied for use in Sections 2.2 to 2.6.

Assumptions common to each device in the cycle are that the steady-flow condition eliminates both time derivatives $\mathrm{d}m_{\mathrm{CV}}/\mathrm{d}t$ and $\mathrm{d}E_{\mathrm{CV}}/\mathrm{d}t$, changes in potential energy are neglected, so $\Delta\mathrm{pe} = 0$, and changes in kinetic energy are neglected, so $\Delta\mathrm{ke} = 0$. Application of these assumptions to the basic mass and energy balance equations results in

$$0 = \sum_{\text{inlets}} \dot{m}_{\mathrm{i}} - \sum_{\text{outlets}} \dot{m}_{\mathrm{o}} \qquad \text{and} \qquad 0 = \dot{Q} - \dot{W} + \sum_{\text{inlets}} (\dot{m}h)_{\mathrm{i}} - \sum_{\text{outlets}} (\dot{m}h)_{\mathrm{o}}. \tag{1}$$

Equation (1) shows the standard sign convention used throughout this paper; that is, heat transfer *into* the system is considered positive, while work transfer *out of* the system is considered positive.

2.2 Compressor

Detailed compressor models for predicting compressor performance are not required for the purposes of test block modeling. Instead, the performance of the compressor is calculated by the model using data from compressor maps (Gessler, 2014). These compressor maps are developed by the company either experimentally for existing compressors or numerically—using other compressor design tools, from basic one-dimensional methodologies to full three-dimensional CFD—for new compressor designs.

A user of the model can select an operating point on the compressor map, and with specification of the suction (inlet) conditions, the discharge (outlet) state of the compressor is fixed. The compressor maps use the dimensionless coefficients of flow, pressure head, velocity, and efficiency (Θ, Ω, Ma, and η_s, respectively) to generalize machine characteristics. The definitions of these coefficients are presented by Gessler (2014).

The four map parameters for the desired operating point (Θ, Ω, Ma, and η_{map}), specified suction conditions (T_{i} and p_{i}), and machine characteristics (D, b, Θ_{peak}, and η_{peak}) allow the model to compute the discharge conditions (T_{o} and p_{o}) and mass flow rate $\dot{m}$. Assuming that the compressor is well-insulated, $\dot{Q} = 0$, leaves $\dot{W}$ as the sole remaining unknown in the compressor energy balance. This value is one of the required outputs of the model.

2.3 Orifice Flow Meter

The ASME PTC 19.5 standard (American Society of Mechanical Engineers, 1972) presents correlations relating the orifice differential pressure to the flow rate for flow measurement purposes. In the model, the flow rate is known and the differential pressure is predicted in order to facilitate orifice selection. The relationships from PTC 19.5 for flange taps are used to predict the orifice discharge coefficient, C, which is used in Eq. (3). These relationships are also used in the data analysis calculations for the 1.1 MW test block's three flow measurement stations.

The model also has provisions for choked flow, which may occur when running the orifice selection routine over large

flow ranges with the smaller orifices. From Munson et al. (2009),

$$p_{\text{o,choked}} = p_{\text{i}} \left(\frac{2}{\gamma + 1} \right)^{\gamma/(\gamma-1)}, \tag{2}$$

where γ is the ratio of specific heats, c_p/c_v. If $p_{\text{o,choked}} > p_{\text{o,free}}$, where subscript free denotes the un-choked outlet pressure, then the flow is said to be choked. The model selects the larger of the two pressures to continue calculations. Finally, the compressible orifice equation is used to relate the differential pressure to the mass flow rate:

$$\dot{m} = CYA_d \sqrt{2\rho_{\text{i}} \Delta p}. \tag{3}$$

The orifice is modeled as a rigid, well-insulated control volume with no shaft work. So $\dot{Q} = \dot{W} = 0$, and thus $h_{\text{o}} = h_{\text{i}}$ for the orifice.

2.4 Condenser

The condenser has two flow streams: a refrigerant stream and a water stream. These streams are unmixed, so the mass balances at steady flow are trivial, and $\dot{m}_{\text{r}}$ and $\dot{m}_{\text{w}}$ are used to simplify the notation for the refrigerant and water streams, respectively.

In the condenser, both the water and refrigerant streams are modeled as having constant pressure. The condenser is modeled as a rigid control volume with no shaft work so that $\dot{W} = 0$. It is also assumed to be well-insulated so that the heat transfer across the external boundary $\dot{Q} = 0$. The internal heat transfer is modeled using the NTU-effectiveness method derived by Incropera et al. (2007); this section contains the pertinent results.

For the condenser in the gas test block refrigeration cycle, the refrigerant is always the hot fluid and the water is always the cold fluid. Therefore, the heat capacities for the hot and cold flow streams are $C_h = \dot{m}_{\text{r}} c_{p,\text{r}}$ and $C_c = \dot{m}_{\text{w}} c_{p,\text{w}}$, where the specific heats are evaluated at the inlet conditions of each flow stream. Although the specific heats vary slightly with temperature, the impact of assuming constant specific heats is negligible. In addition, evaluating specific heats at the inlet temperature greatly simplifies the problem since the outlet temperatures are initially unknown. The NTU for the condenser is defined by

$$\text{NTU} = \frac{UA}{C_{\text{min}}}, \tag{4}$$

where UA is the overall heat transfer coefficient determined from experimental data.

In the NTU-effectiveness method, the heat transfer is modeled in terms of the effectiveness, ε, and the theoretical maximum heat transfer rate, $\dot{Q}_{\text{max}}$, which represents the performance of heat exchanger with infinite surface area. The effectiveness is used to determine the actual heat transfer rate $\dot{Q}$, which is given by $\dot{Q} = \varepsilon \dot{Q}_{\text{max}}$. For a phase-change application such as the condensation process, the effectiveness ε is defined as

$$\varepsilon = 1 - \text{e}^{-\text{NTU}}, \tag{5}$$

while the maximum theoretical heat transfer rate $\dot{Q}_{\text{max}}$ is calculated using

$$\dot{Q}_{\text{max}} = \dot{m}_{\text{r}} (h_{\text{r,i}} - h_{\text{r},T=T_{\text{w,i}}}), \tag{6}$$

which represents fully condensing and cooling the refrigerant stream to the inlet water temperature.

Finally, the enthalpies of the water and refrigerant exiting the condenser can be determined from an energy balance for each flow stream:

$$0 = -\dot{Q} + \dot{m}_{\text{r}} (h_{\text{r,i}} - h_{\text{r,o}}) \qquad \text{and} \qquad 0 = \dot{Q} + \dot{m}_{\text{w}} (h_{\text{w,i}} - h_{\text{w,o}}). \tag{7}$$

Any other properties of the water and refrigerant exiting the condenser, such as temperatures, can be determined based on the known pressures and enthalpies.

2.5 Cooling Tower

The gas test block has multiple rooftop cooling towers to reject energy from the cycle to the outdoor air. To simplify the model, these physical cooling towers are lumped into a single component. Additionally, experimental data for validation are only available on an overall basis and not for each individual tower. The aggregated cooling tower has

two primary flow streams: a water stream requiring cooling and outdoor air, which is treated as a mixture of air and water vapor. These flow streams mix in the cooling tower and a portion of the water stream evaporates into the air-water vapor mixture. By convention, the mass balance for the air-water vapor mixture is written in terms of the dry air mass flow rates, which are equal for a steady-flow system: $\dot{m}_{a,i} = \dot{m}_{a,o}$. As in the condenser model, the notation $\dot{m}_a$ is used throughout for simplicity. For a mass balance on the water stream, an additional term, $\dot{m}_{w,evap}$, accounts for the water evaporated into the moist air stream, so the mass balance is

$$\dot{m}_{w,i} = \dot{m}_{w,o} + \dot{m}_{w,evap}, \tag{8}$$

where the water lost to evaporation is given by

$$\dot{m}_{w,evap} = \dot{m}_a(\omega_{a,o} - \omega_{a,i}). \tag{9}$$

In Eq. (9), $\omega_{a,o}$ and $\omega_{a,i}$ represent the absolute humidity ratio of the air-water vapor mixture at the cooling tower outlet and inlet, respectively.

Braun et al. (1989) developed correlations which are used to apply the NTU-effectiveness method to the cooling tower. First, the saturation specific heat, c_s, is approximated by

$$c_s = \frac{h_{a,s,i} - h_{a,s,o}}{T_{w,i} - T_{w,o}}, \tag{10}$$

where subscript s indicates that the enthalpy is to be evaluated for a saturated air-water vapor mixture. An effective mass flow rate, m^*, is defined as

$$m^* = \frac{\dot{m}_a}{\dot{m}_{w,i} c_{p,w}/c_s}, \tag{11}$$

where the water specific heat, $c_{p,w}$, is evaluated at the inlet conditions. The number of transfer units (NTU) for the cooling tower is calculated using a semi-empirical approach:

$$\text{NTU} = c\left(\frac{\dot{m}_{w,i}}{\dot{m}_{a,i}}\right)^{1+n}, \tag{12}$$

where c and n are empirically determined constants for the cooling tower. The cooling tower effectiveness, ε_a, is then defined as

$$\varepsilon_a = \frac{1 - \exp\big(-\text{NTU}(1-m^*)\big)}{1 - m^* \exp\big(-\text{NTU}(1-m^*)\big)}. \tag{13}$$

Analogous to the heat transfer for the condenser, the heat transfer for the air-water vapor stream is $\dot{Q} = \varepsilon_a \dot{Q}_{max}$, where the maximum possible heat transfer, $\dot{Q}_{max}$, is calculated by assuming that the outlet air is fully saturated at the inlet water temperature:

$$\dot{Q}_{max} = \dot{m}_a(h_{a,s,T=T_{w,i}} - h_{a,i}). \tag{14}$$

The outlet air state is then calculated using $\dot{Q} = \dot{m}_a(h_{a,o} - h_{a,i})$. Finally, the outlet water temperature is given by

$$T_{w,o} = T_{w,i} - \frac{\dot{m}_{a,i}(h_{a,o} - h_{a,i})}{\dot{m}_{w,i} c_{p,w}}. \tag{15}$$

2.6 Minor Components

The actual gas test block cycle has a complicated arrangement of numerous valves and spray nozzles which simultaneously throttle and mix the condensed refrigerant stream with the bypassed refrigerant stream to reestablish the compressor suction conditions. For the purposes of a one-dimensional model, this complex arrangement may be separated into three distinct processes: throttling the condensed refrigerant stream to the cycle's low pressure (suction pressure); throttling the hot gas bypass refrigerant stream to the cycle's low pressure; and mixing the two refrigerant streams in the correct proportions to achieve the specified test suction conditions.

The expansion devices, mixing chamber, and flow split following the orifice flow meter are modeled as rigid control volumes with no shaft work ($\dot{W} = 0$). Additionally, they are assumed to be well-insulated ($\dot{Q} = 0$). It is assumed that the flow split and mixing process both occur at constant pressures. Therefore, the two balances on the mixing chamber constrain the division of flow between the condensed and bypassed streams by requiring that their mixing re-establishes the specified suction condition.

3. SOLUTION METHODOLOGY

The equations developed in Section 2 were implemented in Engineering Equation Solver (EES). This software package provides thermophysical property data, unit checking, a graphical user interface (GUI) framework, and an automatic equation blocking scheme for iteratively solving systems of simultaneous equations. These features, along with compressor and test engineers' familiarity with the program, make EES an ideal choice for implementation of the gas test block model. The model is implemented using an EES module for each device in the cycle, which facilitates a code structure analogous to the physical system and will simplify code maintenance for future modifications or improvements to the model.

One of the goals of the project is to provide a tool for selecting the best flow measurement orifice for conducting tests over a user-input range of operating points. Achieving this goal requires running the model with each orifice configuration at multiple operating points within the user-specified range of conditions. Because the EES software restricts the number of variables that can be stored, it is not feasible to store the properties at each point in the cycle for multiple operating points. However, in some situations, the user would like to know detailed information about the gas test block at a single operating point. For this reason, two EES programs were developed, each sharing a common code base but providing different outputs.

The first program computes results for the entire cycle, but only for a single operating point at a time. This program is used to evaluate the feasibility of achieving the desired test conditions under specified outdoor air conditions. If the cooling towers cannot transfer sufficient heat to fully condense the refrigerant, then the gas test block cannot operate at steady state. If the calculated air mass flow rate through the model cooling tower exceeds the nominal air flow rate for the cooling towers, the operating condition is predicted to be infeasible at the given outdoor air conditions.

The second program has the capability to evaluate and store orifice and compressor model results for multiple operating points. The orifice selection program calls only the compressor and orifice modules of the main code, which are the only modules required to model the orifice differential pressure. In order to obtain accurate mass flow measurements, the orifice differential pressure must be within the range 2.50–250 kPa (10–990 inH_2O) (Graham, 2006). Therefore, it can be used to evaluate the suitability of different flow measurement orifices over a specified range of test conditions. Simplifying the model to only two modules keeps the orifice selection program within the maximum number of variables allowed by EES. A flowchart of the orifice selection algorithm is shown by Gessler (2014).

The complete EES code is displayed and briefly explained in Appendix A of Gessler (2014). This code is used as the basis for both the complete cycle program and the orifice selection program. Each of these programs use the diagram window functionality of EES to provide a user interface for the model as described by Gessler (2014).

4. RESULTS AND DISCUSSION

A crucial component of any modeling effort is to confirm that the model agrees with experimental data to a level appropriate for the intended application. This validation process confirms the appropriateness of the simplifying assumptions made during the model development. For the 1.1 MW gas test block, experimental data are available for numerous tests conducted in July 2005 and November 2012. The test data from the project sponsor were obtained using the guidelines in Graham (2006) and in accordance with Gerber (1998).

4.1 Comparison of Experimental and Model Results

This section presents the validation results for the complete cycle program. More in-depth discussion of the results is presented by Gessler (2014). The results for each condition considered are summarized in parity plots, Figs. 3 and 4, alongside related discussion. Each parity plot illustrates perfect agreement between modeled and experimental results with a solid line and $\pm 5\%$ difference bounds with dashed lines.

Compressor Module Because the compressor module is based on compressor characteristics that are determined through experimental testing, the results are expected to show excellent agreement. Indeed, the maximum percent difference for the compressor discharge pressure is 0.018%. Similarly, the maximum difference for the compressor discharge temperature is 0.6 °C, or 0.2% by using an absolute temperature scale. The error is still acceptable in this

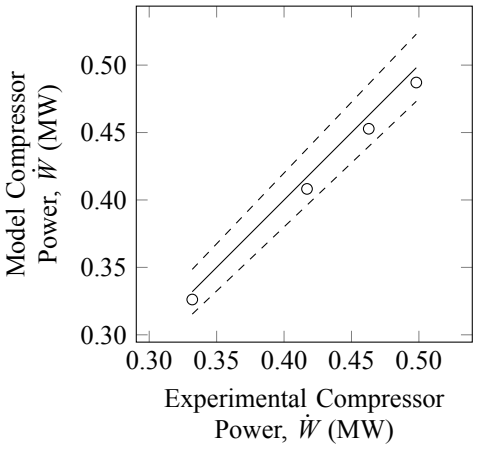

Figure 3: Compressor gas power parity plot.

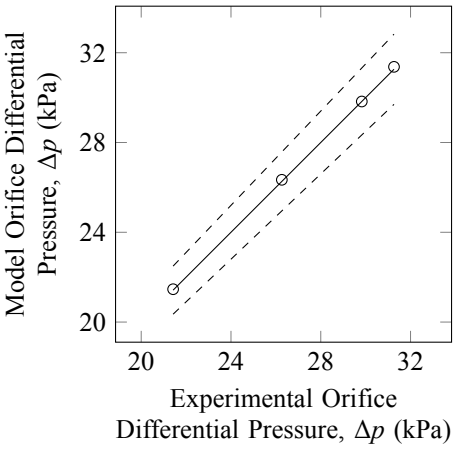

Figure 4: Orifice differential pressure parity plot.

case, but is larger because of a difference in the compressor Reynolds number computation. The sensitivity of the model to this Reynolds number and its impact on model outputs is studied further in Section 4.2.

The compressor gas power is shown in Fig. 3. This required output of the model agrees with the experimental results to within 2.5%. The compressor Reynolds number calculation affects the gas power slightly, because the lower discharge temperature predicted by the model corresponds to a lower discharge enthalpy, and the gas power is directly proportional to the increase in enthalpy across the compressor. Another possible source of error is the assumption of an adiabatic compressor. Heat transfer from the compressor casing to the ambient environment would increase the predicted gas power requirement for the test block.

Orifice Module The orifice differential pressure is the primary output of the model in the orifice selection program. The differential pressure is used to evaluate the suitability of different orifice diameters for the range of test conditions specified. As shown in Fig. 4, the model shows excellent agreement with the experimental results, with a maximum percent difference of 0.35% for the conditions considered for validation. This shows that the orifice selection program will be an excellent aid to simplify the calculations required to plan a set of tests.

The EES model generates a plot illustrating the differential pressure for each orifice over the specified range of flow conditions. The results are plotted on semi-logarithmic axes for clarity at both high and low differential pressures. A typical set of results is shown in Fig. 5. The ordinate axis limits correspond to the acceptable differential pressure range for flow measurement, 2.50–250 kPa (10–990 inH_2O). Therefore, a particular orifice is acceptable only if its differential pressure curve remains within the axis limits over the desired range of flow coefficients.

As discussed in Section 2.3, the model considers the possibility of choked flow through the orifices by comparing the predicted differential pressure to the maximum differential pressure, which occurs with choked flow. If choked flow is predicted, it will limit the mass flow rate, and thus the specified operating point cannot be achieved on the gas test block with the specified orifice. Sample results for choked flow are shown in Fig. 6. For this scenario, orifices 1 and 2 do not reach choked conditions, while orifices 3–14 experience choked flow and reach the maximum differential pressure. Figures 5 and 6 illustrate how the model will enable engineers to quickly select orifices for testing.

Condenser Module In the condenser, the outlet pressure is recorded in the experimental data. This allows the constant pressure assumptions in the flow split and condenser modules to be evaluated. The model results for condenser pressure deviate from the experimental results by a maximum of 0.15%. Therefore, the constant pressure assumptions in the components and connecting piping are reasonable for the 1.1 MW gas test block.

The condenser refrigerant liquid temperature is also recorded, and it can be used to calculate the degree of subcooling in the condenser. The comparison of modeled and measured liquid temperature is used to confirm that the condenser

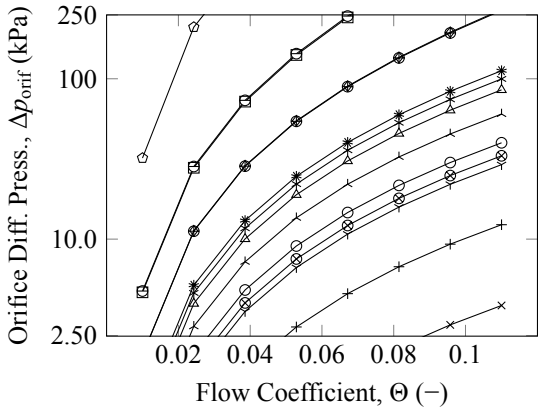

Figure 5: Typical orifice selection results. The axis limits correspond to the acceptable measurement range, 10–990 inH_2O.

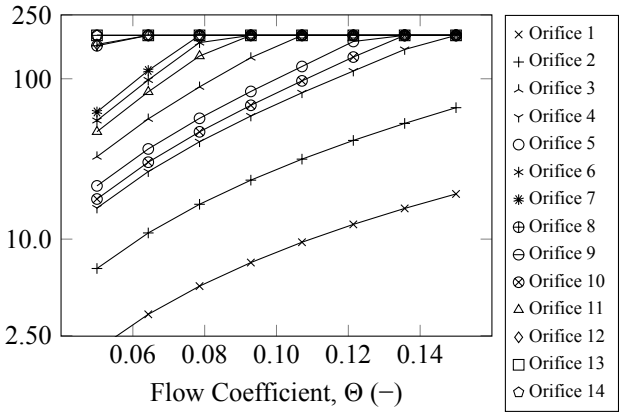

Figure 6: Orifice selection program results showing choked flow for orifices 3–14. For these conditions, only orifice 2 is acceptable over the entire range of flow coefficients.

model provides an accurate representation of the complex heat transfer taking place. The results for the condenser refrigerant liquid temperature have a maximum deviation from experimental results of 0.9 °C.

Cooling Tower Module The average condenser water temperature provides insight into the performance of both the cooling tower and condenser. Despite many assumptions concerning the parameters *UA*, *c*, and *n* (Sections 2.4 and 2.5), the results agree with the experimental data to within 3 °C.

Because the parameters are currently empirically-based, these differences are liable to increase at operating conditions further away from the conditions recorded in the experimental data. Recall from Section 2.5 that several cooling towers on the physical test block are lumped into a single cooling tower for the purposes of the model. In addition, neither the cooling tower fan speeds nor the condenser water flow rate are recorded as part of the test data, so average values are currently used. This is discussed further in Section 4.2.

4.2 Sensitivity Analysis

This section shows that the differences between Reynolds numbers calculated in the compressor and orifice modules (Section 4.1) and calculated based on experiments have a negligible impact on the important output variables. It also studies the impact of the condenser water flow rate on the water temperatures and cooling tower flow rate requirements, because of the uncertainty involved in estimating the water flow rate. The model currently uses an average water flow rate calculated from test data. This is because a bypass loop is used on the block, but no data on the bypass loop flow rate or condenser loop flow rate are currently recorded.

In the compressor, the Reynolds number is used in the calculation of the isentropic efficiency, which affects the discharge temperature and thus the gas power of the compressor. The discharge pressure should not be influenced. To study the extent of these effects, the Reynolds number was artificially adjusted by several different percentages, and the compressor module outputs were recorded. These results are summarized in Fig. 7. The gas power is affected by a maximum of 970 kW; therefore, the error in the compressor gas power (Fig. 3) is mostly attributable to the adiabatic assumption of Section 2.2.

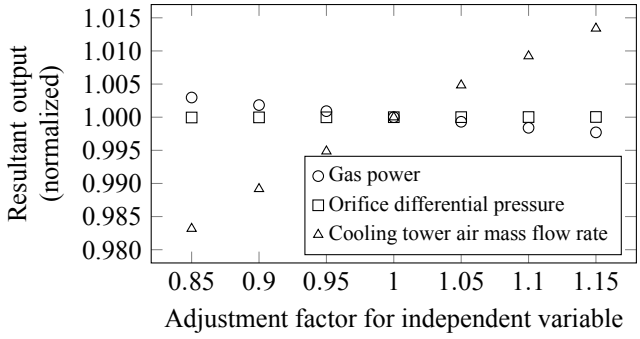

Figure 7: Summary results of the sensitivity analyses.

The orifice Reynolds number shows the same discrepancy as the calculation at the compressor. In the orifice, the Reynolds number has a slight effect on the coefficient of discharge, *C*, calculated using the ASME PTC 19.5 correlations

of Section 2.3. The orifice Reynolds number was adjusted to study the significance of these effects on orifice differential pressure, and they are even less significant than the effects on the compressor module. Figure 7 displays the results, and it is clear that the impact is well under the level of uncertainty in the measurements on the gas test block.

In the condenser, an average water flow rate calculated using experimental results is used in the absence of true flow rate measurements. Changes in the water flow rate will influence the water temperatures at the condenser and, most importantly, the required air mass flow rate in the cooling tower. Figure 7 shows the impact of changing the condenser water flow rate on the cooling tower air mass flow rate. For a 30% change in water flow rate, the cooling tower air flow rate changes by only 3%. The water temperatures are affected slightly, but overall, the cooling tower mass flow rate is fairly insensitive to the specified condenser water mass flow rate.

5. CONCLUSIONS AND RECOMMENDATIONS

This section contains a summary of the research work presented in this paper and discusses the resulting conclusions. In addition, it contains recommendations for future improvements to the model and test block data acquisition. These data acquisition improvements would enable more extensive validation of the model, which in turn would improve the accuracy of the model by guiding the selection of empirical parameters.

5.1 Conclusions

Based on the results presented and discussed in Section 4, the model meets the two primary goals of predicting whether test conditions are feasible and assisting in orifice selection. These goals were accomplished by predicting the air mass flow rate in the cooling tower and predicting the differential pressure across the orifice. For the validation cases of Section 4, the maximum percent difference between model and experimental results is 2.5%, indicating that the model is quite accurate given the number of assumptions involved. The model's prediction of cooling tower air flow rate cannot be assessed because it is not measured during tests, but the primary output variable for orifice selection, the orifice differential pressure, agrees with the experimental results to within 0.35%. It should be noted, however, that the validation encompassed only a small range of test points and weather conditions, from which several of the parameters in the model are defined. Results for operating conditions far removed from the validation data may vary. Methods for correcting this shortcoming of the model are discussed in Section 5.2.

5.2 Recommendations

As noted in Section 4 and Section 5.1, the condenser and cooling tower modules of the model make significant assumptions to determine the parameters that characterize their performance. These parameters include the overall heat transfer coefficient for the condenser, UA, and the two characteristic parameters for the cooling tower model's calculation of NTU, c and n. To improve these portions of the model, several data collection recommendations are prudent.

First, the cooling tower fan speeds should be recorded as part of each test. Combined with fan curves for the cooling towers installed on the block, records of the fan speeds will allow calculation of the cooling tower model parameters c and n. This will enhance the accuracy of the cooling tower model and extend the range of test conditions over which its accuracy is acceptable. At present, the model uses typical values for these parameters from Braun et al. (1989).

Similarly, a means to determine the condenser water flow rate would greatly improve the accuracy of calculations for the condenser overall heat transfer coefficient, UA. As discussed in Section 4.2, the condenser water pump drives the flow through both a bypass loop and the condenser loop. With the current instrumentation setup, the division of flow between these loops is unknown.

Other potential improvements to the model concern the adiabatic assumption in the compressor, which results in under-prediction of the compressor gas power, as discussed in Section 4.1. A model of the heat transfer from the compressor casing to the ambient conditions is likely to improve this prediction. Because of the modular construction of the model, it will be relatively straightforward to implement this improvement or any others.

The data collection additions on the gas test block may prove more difficult to complete, but if these are possible, they would expand the validation possibilities and allow for better estimation of the characteristic parameters in the model. In addition, the model serves its intended purpose as it currently stands. Therefore, it is expected that the thermodynamic model will serve as a useful tool for conducting efficient compressor tests at the gas test block facility.

NOMENCLATURE

Symbol	Description	Units
A	Area	m^2
c_p, c_v, c_s	Specific heats, const. pressure, const. volume, and saturation, respectively	$kJ\,kg^{-1}\,K^{-1}$
h	Specific enthalpy, $h = u + pv$	$kJ\,kg^{-1}$
m	Mass	kg
Ma	Machine Mach number, $\mathcal{V}_{tip}/a$	–
NTU	Number of transfer units	–
p	Pressure	kPa
Q	Heat transfer	kJ
s	Specific entropy	$kJ\,kg^{-1}\,K^{-1}$
T	Temperature	°C, K
t	Time	min
v	Specific volume	$m^3\,kg^{-1}$
$\mathcal{V}$	Velocity magnitude	$m\,s^{-1}$
W	Work transfer	kJ
Y	Expansion factor	–

Greek Symbols		
ε	Heat exchanger effectiveness, $\dot{Q}/\dot{Q}_{max}$	–
η	Efficiency	–
γ	Ratio of specific heats, $\gamma = c_p/c_v$	–
Ω	Isentropic head coefficient, $g_c\Delta h_s/a^2$	–
ω	Absolute humidity ratio	kg_w/kg_a
ρ	Density, $1/v$	$kg\,m^{-3}$
Θ	Flow coefficient, $\dot{V}/aD^2$	–

Subscripts	
a	Air-water vapor mixture
CV	Control volume
i	Inlet conditions
o	Outlet conditions
r	Refrigerant
s	Saturated
w	Water
s	Isentropic

REFERENCES

American Society of Mechanical Engineers (1972). ASME PTC 19.5-1972: Flow Measurement. Technical report, The American Society of Mechanical Engineers, New York.

Braun, J. E., Klein, S., and Mitchell, J. (1989). Effectiveness models for cooling towers and cooling coils. *ASHRAE Transactions*, 95:164–174.

Çengel, Y. A. and Boles, M. A. (2011). *Thermodynamics: An Engineering Approach*. McGraw Hill, New York, 7 edition.

Dirlea, R., Hannay, J., and Lebrun, J. (1996). Testing of refrigeration compressors without condensation. In *Proceedings of International Compressor Engineering Conference at Purdue University*, number 1113, pages 241–246, Belgium. University of Liége.

Gerber, G. J. (1998). ASME PTC 10-1997: Performance Test Code on Compressors and Exhausters. Technical report, The American Society of Mechanical Engineers, New York.

Gessler, P. D. (2014). A one-dimensional model of a closed-loop refrigeration test block for centrifugal compressors. M.S. Thesis, Marquette University.

Graham, E. (2006). Operating limits, 1500 hp compressor test facility, test facility #104, building 10. Technical Report EF-104-06, York International Corporation.

Iancu, F. V. (2012). One-dimensional model of a closed loop refrigeration test block for compressors. Internal whitepaper, Johnson Controls, Inc.

Incropera, F. P., DeWitt, D. P., Bergman, T. L., and Lavine, A. S. (2007). *Introduction to Heat Transfer*. John Wiley and Sons, Inc., Hoboken, NJ, 5 edition.

McGovern, J. (1984). Analysis of a refrigerant compressor load stand incorporating hot gas bypass and a single full condensation heat exchanger. In *Proceedings of the International Compressor Engineering Conference at Purdue University*, number 491, pages 468–477, Dublin, Ireland. Trinity College.

Munson, B., Young, D., Okiishi, T., and Huebsch, W. (2009). *Fundamentals of Fluid Mechanics*. Wiley, Hoboken, NJ, 6 edition.

Sahs, L. J. and Mould, Jr., H. W. (1956). Apparatus for testing refrigeration compressors. U.S. Patent 2733600, Fedders-Quigan Corporation, Buffalo, NY.

ACKNOWLEDGMENT

The authors would like to acknowledge financial support and technical recommendations provided throughout the project by Mr. John Trevino, Jr. and Mr. Steven T. Sommer of Johnson Controls, Inc. We also thank Mr. Florin Iancu for his work defining the project in its early stages.